Band offset of the ZnSe–ZnTe superlattices: A fit to photoluminescence data by k·p theory

Y. Rajakarunanayake, R. H. Miles, G. Y. Wu, and T. C. McGill
California Institute of Technology, Pasadena, California 91125

(Received 1 February 1988; accepted 4 May 1988)

The ZnSe–ZnTe superlattices have attracted considerable attention as possible blue/green light emitters. Although these superlattices have been successfully fabricated and show intense photoluminescence, there are many basic issues about this system which still remain unresolved. The most important of them is the value of the valence band offset between ZnSe and ZnTe. We have studied the band structure of ZnSe–ZnTe superlattices. Our calculations are based on second order **k·p** theory and include the effects of strain and spin-orbit splitting on the superlattice band structure. We have investigated the dependence of the superlattice band gap on the valence band offset. Based on the assumption that the photoluminescence from the superlattice corresponds to a bound exciton at a Te_i isoelectronic center in ZnSe, we have fit the experimental photoluminescence data with **k·p** theory to obtain the best value of the valence band offset. The value we find is 0.97 ± 0.10 eV. Alternatively, assuming that the photoluminescence was due to band-to-band transitions we obtain a valence band offset of 1.20 ± 0.13 eV. We have also calculated the superlattice band gap as a function of the constituent material layer thicknesses for the first valence band offset quoted. We expect these results to be important in gaining an understanding of the value of the valence band offset, and the nature of the photoluminescence from this system.

I. INTRODUCTION

ZnSe and ZnTe are II–VI semiconductors which have direct band gaps in the blue–green region of the spectrum. Thus devices based on these materials offer great promise as candidates for short wavelength semiconductor optoelectronics. The recent advances in epitaxial crystal growth techniques such as molecular-beam epitaxy (MBE) have enabled the fabrication of novel device structures based on II–VI semiconductors for applications in the optoelectronics arena. One such example is the ZnSe–ZnTe superlattice.

The ZnSe–ZnTe superlattice is an interesting structure as it offers considerable promise as a means of producing tunable light emitters by variation of the constituent material layer thicknesses. It is thought that these superlattices would be particularly promising in producing blue light emitting diodes (LED's) and short wavelength semiconductor lasers.[1–5] The successful growth of these superlattices has been achieved by a variety of methods such as MBE,[1–3] hot-wall epitaxy (HWE),[4,5] and atomic-layer epitaxy (ALE).[6,7] Characterization studies done on ZnSe–ZnTe superlattices by a variety of methods such as reflection high-energy electron diffraction (RHEED),[3] transmission electron microscopy (TEM),[8,9] x-ray diffraction measurements,[5] and photoluminescence (PL)[1,4] reveal that high-quality interfaces have been achieved. The photoluminescence from these superlattices has been studied by Kobayashi *et al.*[1] on samples grown by MBE, and by Kuwabara *et al.*[4] on samples grown by HWE. Intense green/red photoluminescence has been observed from these superlattices at 71 K. While it seems that these superlattices can be grown successfully and offer promise as light emitters, there is much work that needs to be done on the applicability of these superlattices in optoelectronics devices, as well as resolving basic issues such as the value of the heterojunction band offset between ZnSe and ZnTe.

In this paper we have performed band structure calculations for this superlattice using second order **k·p** theory including strain and spin-orbit effects. We have investigated the band offset of the ZnSe–ZnTe system by comparing our results with the photoluminescence data.[1,10] In Sec. II we review the wide range of predicted values of the valence band offset, and the various implications of having a large or small offset. In Sec. III we describe the details of the **k·p** band structure calculations. In Sec. IV we examine the effects of strain and valence band offset on the superlattice band structure. The experimental photoluminescence peaks have been analyzed based on two assumptions. In the first case, we attribute the photoluminescence from the ZnSe–ZnTe superlattices to a bound excitonic emission band that exists in Te-doped ZnSe, and perform a fit to the experimental data to arrive at a value for the valence band offset. In the second case we obtain the best fit for the valence band offset assuming that the photoluminescence is due to band-to-band transitions.

II. BAND OFFSET

One of the key parameters that determines the band gap of the superlattice is the valence band offset between ZnSe and ZnTe. In Fig. 1 we have shown a schematic type II band alignment. The value of the valence band offset used for this figure is taken from Harrison.[11] Almost all of the predictions for the valence band offset place the valence band edge of ZnSe below that of ZnTe. The band gaps of ZnSe and ZnTe at 77 K are 2.81 and 2.36 eV, respectively.[12] These numbers imply that if the valence band offset $E_V^{\mathrm{ZnTe}}-E_V^{\mathrm{ZnSe}}$ is <0.45 eV the superlattice band alignment would be type I at this

 0734-211X/88/041354-06$01.00

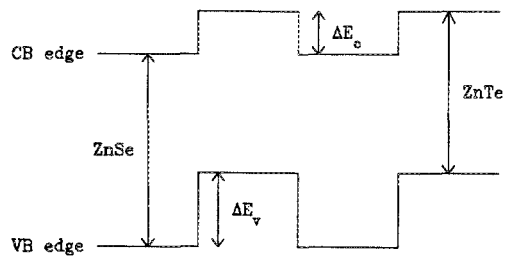

FIG. 1. Schematic diagram of a type II superlattice band alignment, indicating the relative positions of the ZnSe/ZnTe conduction and valence band edges. The values ΔE_V and ΔE_C are the valence band and conduction band offsets, respectively.

temperature. However, in the case when the valence band offset is higher than 0.45 eV, the band alignment would be type II. In typical type II systems, the band gap of the superlattice is usually less than that of either one of the constituent bulks. Thus a type II band alignment is not favorable for the fabrication of blue optoelectronic devices. However, there are predictions for the valence band offset that agree with type I and type II alignments.

If electrical injection of minority carriers is to be used in generating carriers for pumping ZnSe/ZnTe based optoelectronics devices, then controlling the doping characteristics of these materials is very important. ZnSe can be readily doped *n* type and ZnTe can be readily doped *p* type. It is usually difficult to change this conduction type. Since many native defects are produced as a consequence of dopant atom incorporation, it is exceedingly difficult to control the conductivity. Thus the fabrication of *p–n* homojunctions for efficient minority carrier injection is quite a challenge. Recently it has been reported that low-resistivity *p*-type ZnSe can be achieved by lithium doping.[13]

On the other hand, the *n*-ZnSe/*p*-ZnTe heterojunction offers a possibility for electrical injection of carriers. The valence band offset of Fig. 1 acts as the barrier for hole injection from ZnTe to ZnSe, and the conduction band offset acts as the barrier for electron injection from ZnSe to ZnTe. Ideally, one would like the carriers to recombine in the wider band gap material (ZnSe) giving out light across the higher energy gap. From Fig. 1, we see that the conduction band offset is about 0.45 eV lower than the valence band offset. Thus, electron injection into ZnTe is a much more likely process to happen than the injection of holes into ZnSe. It has been suggested that doping the ZnSe layers with Mn near the interfaces might reduce the electron current.[14,15] Nevertheless, a large valence band offset would still make it difficult to thermally inject holes into ZnSe. If the valence band offset is large, then the radiative recombination of carriers at the heterojunction may have to be achieved from a different process (for example, recombination *across* the junction, tunneling injection.) However, recent theories of Harrison and Tersoff[16] and measurements by Katnani and co-workers[17] have arrived at small valence band offsets suggesting that thermal injection of holes from ZnTe into ZnSe may be a possibility. Clearly, the magnitude of the valence band offset will play a decisive role in determining the type of device required for efficient light emission.

The values quoted for the valence band offset span a wide range (0.3–1.2 eV). In Fig. 2 we have indicated the relative positions of the valence band edges of ZnSe and ZnTe for some of these predictions. Harrison and Tersoff[16] predict a valence band offset of 0.29 eV. Katnani and co-workers[17] report a measured valence band offset of 0.43 eV. The value labeled Milnes and Feucht[18] was obtained by using the electron affinity difference to give the conduction band offset. The prediction of Harrison (1977)[11] is 1.08 eV. The most recent value predicted by Van de Walle places the valence band offset at 1.20 eV.[19] Thus, while the valence band offset is a key parameter in determining the properties of ZnSe–ZnTe superlattices and heterojunctions, its value remains uncertain.

III. THEORY

The bulk band structure of ZnTe and ZnSe is calculated using Kane's eight band model.[22] The method employed is similar to the previous work of Wu and McGill[23] on HgTe–CdTe superlattices. The calculation of the complex band structure of the bulk layers as well as the calculation of the superlattice band structure in the envelope function approximation was performed according to the method outlined by Smith and Mailhiot.[24] In this paper we only briefly review the details of the calculation. The eight bands that make up the zone center basis set are the four Γ_8 bands (light hole and heavy hole bands), two Γ_7 bands (spin-orbit split-off bands) and two Γ_6 (conduction bands). We have taken the param-

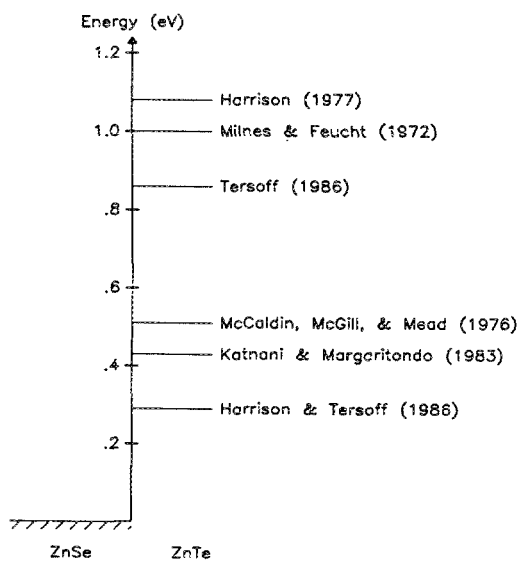

FIG. 2. The relative position of the ZnTe valence band edge with respect to that of ZnSe, according to a number of different theories. The value labeled Harrison and Tersoff (1986) was obtained from Ref. 16. The value labeled Katnani and Margaritondo (1983) was obtained from Ref. 17. The value labeled McCaldin, McGill, and Mead (1976) was obtained from Ref. 20. The value labeled Tersoff (1986) was obtained from Ref. 21. The value labeled Milnes and Feucht (1972) was obtained by using the electron affinity difference to give the conduction band offset (after Ref. 18). The value labeled Harrison (1977) was obtained from Ref. 11. The value labeled Van de Walle (1988) was obtained from Ref. 19.

eters for our calculations from Lawaetz with the corrections for the 77 K gaps.[12] The values we used were $E_0^{ZnSe} = 2.810$, $E_0^{ZnTe} = 2.364$, $\Delta_0^{ZnSe} = 0.43$, $\Delta_0^{ZnSe} = 0.92$, $E_p^{ZnSe} = 24.2$, and $E_p^{ZnTe} = 19.1$. All of these energies are in eV. Here E_0 and Δ_0 are the fundamental band gap and the spin-orbit splitting, respectively. E_p is related to the P-matrix element by the relation $E_p = 2mP^2/\hbar^2$, where m is the free electron mass. The effects of the higher bands are included through perturbation theory by the use of Luttinger valence band parameters. These parameters were also taken from Lawaetz[12] to be $\gamma_1^{ZnSe} = 3.77$, $\gamma_1^{ZnTe} = 3.74$, $\gamma_2^{ZnSe} = 1.24$, $\gamma_2^{ZnTe} = 1.07$, $\gamma_3^{ZnSe} = 1.67$, $\gamma_3^{ZnTe} = 1.64$, $\kappa^{ZnSe} = 0.64$, $\kappa^{ZnTe} = 0.42$, $q^{ZnSe} = 0.02$, and $q^{ZnTe} = 0.05$. To preserve the isotropy of the bulk bands, we replaced the values of γ_2 and γ_3 of each material by the average of γ_2 and γ_3 listed above and set $q = 0$. In our calculations we have taken the lattice constants of the unstrained bulks to be $a^{ZnSe} = 5.669$ Å and $a^{ZnTe} = 6.104$ Å.[25]

The first step in our calculation is to solve for the complex band structure of the strained bulk layers. Our Hamiltonian is an 8×8 matrix with quadratic dependences in **k**. In the current analysis we have considered the case when $k_{\|} = 0$. This is appropriate since we are only interested in the near band edge properties. Since the samples were grown in the [100] orientation, we have limited our attention to [100] superlattices throughout this work. The complex band structure is obtained by first specifying the energy and then calculating the allowed values of $k_\perp$. The number of allowed solutions of $k_\perp$ is twice the dimension of the Hamiltonian due to the quadratic dependence in $k_\perp$.

In the fabrication of novel semiconductor heterostructures, one can only find a very limited set of lattice matched semiconductor pairs. However, semiconductor pairs such as ZnSe and ZnTe that are not lattice matched can still be grown in thin epitaxial layers with relatively few misfit dislocations if the layer thicknesses are kept smaller than the critical thicknesses. The large lattice mismatch of $\simeq$7.2% that exists between these two semiconductors causes strain to play an important role in determining the characteristics of the ZnSe–ZnTe superlattice.

In our calculations we have assumed that the magnitude of the strain in each layer is given by minimizing the elastic free energy of the structure. This is the so-called free-standing configuration. It is appropriate for most ZnSe–ZnTe superlattices owing to the magnitude of the lattice mismatch; critical thickness models suggest that strain distributions deviating substantially from the free-standing case can be maintained for only a few monolayers.[26] Experimental studies show that superlattices grown well beyond the critical thickness can adopt a relatively defect-free structure in which the in plane lattice constant jumps to that of the free-standing superlattice.[26] This justifies our analysis of ZnSe–ZnTe superlattices with layer thicknesses on the order of 10–20 Å based on the free-standing assumption. Our calculations indicate that the strain effects produced by this large a lattice mismatch can change the positions of the band edges of the superlattice by as much as 100–200 meV relative to their unstrained positions.

Strain effects are easily included in the bulk Hamiltonians by the observation that the elements of the strain tensor ϵ_{ij} transform like $k_i k_j$ in the Kane Hamiltonian. Here i, j label the directions of the axes and k denotes the electronic wave vector. For superlattices grown on [100] orientations, the strain terms due to lattice mismatch appear only as the diagonal components of the strain tensor. We have used a model with four deformation potentials to describe the effects of strain on the bulk band structure. Following the convention of Pikus and Bir,[27] we have defined the three independent parameters a, b, and d to describe the effects of strain on the valence bands. Here a describes the hydrostatic shift in energy originating in the p-like bands due to strain. Uniaxial strains in the [100], and [111] directions are described by b and d, respectively. A parameter c describes the hydrostatic shifts in the s-like energy bands. The values we used were[28,29] $a^{ZnSe} = 1.35$, $a^{ZnTe} = 1.35$, $b^{ZnSe} = -1.20$, $b^{ZnTe} = -1.78$, $d^{ZnSe} = -3.81$, $d^{ZnTe} = -4.58$, $c^{ZnSe} = -2.82$, and $c^{ZnTe} = -2.70$. These deformation potentials are expressed in eV. The elastic constants were taken to be[30] $C_{11}^{ZnSe} = 8.10$, $C_{11}^{ZnTe} = 7.13$, $C_{12}^{ZnSe} = 4.88$, $C_{12}^{ZnTe} = 4.07$, $C_{44}^{ZnSe} = 4.41$, and $C_{44}^{ZnTe} = 3.12$. These elastic constants are expressed in 10^{10} Nm^{-2}.

The superlattice band structure is calculated in the multicomponent envelope function approximation. The eigenstates we find from **k·p** theory can be propagated from one interface to the other within a given bulk layer. However, to match the wave functions across the interface, we have to impose boundary conditions on the wave functions and their normal derivatives. We have made use of the fact that both ZnSe and ZnTe are crystals of zinc-blende symmetry, and thus have zone center wave functions of the same symmetry. Accordingly, we have assumed that there is no mixing of the zone center components as the wave function crosses the interface. This allows us to make the zone center components of each wave function continuous across the interface as we change from one material to the other. The other boundary condition based on the normal derivatives of the zone center components corresponds to making the current density of each wave function continuous across the interface. This simplifies to the condition that net charge accumulation at the interface from each wave function is zero.

Finally we impose the Bloch condition that relates the amplitude of the wave function at a given point in a superlattice unit cell to the amplitude in an adjacent cell at the same corresponding point by a factor of the form $e^{iQ(d_1+d_2)}$. Here d_1 and d_2 are layer thicknesses within a single period of the superlattice, and Q denotes the superlattice wave vector. The Bloch condition can be cast into an eigenvalue problem whose solution would give us the values of the superlattice wave vector Q. In an actual calculation, for each value of k we obtain, we find that k^*, $-k$, and $-k^*$ are also solutions due to the symmetry of the Hamiltonian. This makes it possible to reduce the dimensions of our matrices. The 16 bulk bands we obtain correspond to 4 heavy hold bands, 4 light hole/conduction bands, 4 spin-orbit bands, and 4 bands with very large imaginary wave vectors at all energies of interest. We have neglected the contribution to the superlattice states from this set of pure imaginary bands. This turns out to be a good approximation since the inclusion of the correction

terms from these bands typically changes the wave functions only by about one part in 10^6.

IV. RESULTS

Since strain moves the band edge positions, the effective valence band offset in the superlattice is different from the unstrained offset and depends on the particular strain distribution in the structure. Thus, it is more meaningful to describe the valence band offset as the difference of the valence band edges of the two materials before strain is introduced. The quantity so defined has the advantage of being independent of strain and layer thicknesses, and will be commonly denoted as the band offset in this paper. In our calculations, we obtain the positions of the strained bulk band edges by simply adding the energy shifts due to deformation potential terms to an initial band alignment based on the unstrained band offset.

The above defined unstrained valence band offset is an input parameter to our calculations. An illustrative case is shown in Fig. 3 as the difference between the dashed lines. Here, we have shown the relative alignments of the energy bands for the Harrison[11] value of the valence band offset of 1.080 eV. This value of the band offset was chosen purely for illustrative purposes to discuss the effects of strain on the bulk band structures of ZnSe and ZnTe. The band structures of ZnSe and ZnTe in Fig. 3 were calculated assuming that the magnitude of the strain in each layer was equal to that of a free-standing 15–15 Å superlattice. As described earlier, by a free-standing superlattice we mean a configuration in which the in-plane lattice constant is chosen to minimize the elastic free energy of the structure.

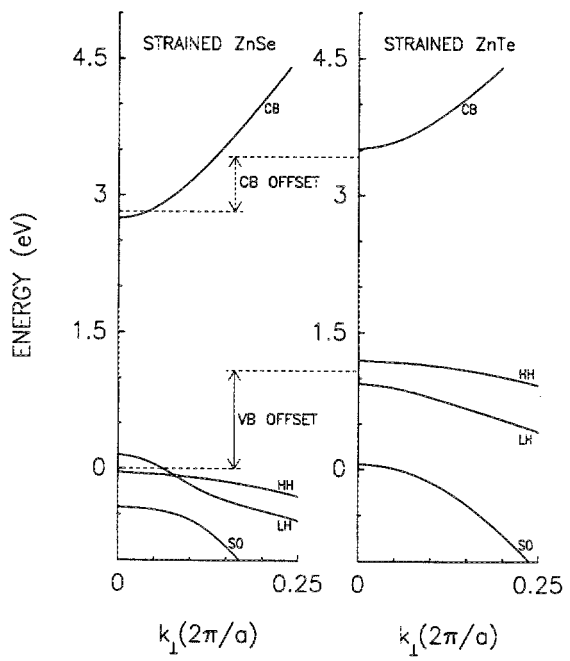

FIG. 3. Band structure of bulk ZnSe and ZnTe including strain appropriate to a 15–15 Å free-standing superlattice. Zero of energy is taken to be the valence band edge of ZnSe before strain is introduced. Harrison's (Ref. 11) valence band offset $E_V^{ZnTe} - E_V^{ZnSe} = 1.080$ eV is used. Dashed lines indicate the positions of the band edges of the unstrained bulks. The band structure shown is along the growth direction [100].

The band structures shown in Fig. 3 correspond to the strained bulks in the [100] direction with $k_\parallel = 0$. We have shown the band structure only up to a quarter of the distance to the Brillouin zone edge along the growth direction of the superlattice. ZnSe layers in the superlattice are under tensile strain, which has the effect of reducing the band gap of this material. Thus the valence bands of ZnSe move up, and the conduction bands move down with respect to their unstrained positions. In addition, the degeneracy of the heavy hole and light hole band is removed by the uniaxial strain. The dashed lines indicate the original positions of the band edges. In the superlattice of Fig. 3, the ZnSe light hole bands are shifted up in energy by 157 meV, while the heavy hole bands shift down in energy by 37 meV. The conduction bands of ZnSe are also lowered by 78 meV for this case. On the other hand the ZnTe layers of the superlattice are under compressive strain. This causes the conduction bands to move up, and the valence bands to move down with respect to their unstrained positions, increasing the band gap of this material. The heavy hole and the light hole bands are also split about their average position due to uniaxial terms. In Fig. 3, the ZnTe heavy hole moves up by 118 meV, the light hole moves down by 135 meV, and the conduction band moves up by 85 meV. We also see that the spin-orbit split-off bands play a more important role in ZnSe than in ZnTe because they are closer to the light hole band in ZnSe.

In Fig. 4 we have shown the dependence of the band gap on the valence band offset for a strained free-standing superlattice. Due to the large range of valence band offsets reported for this system, we have presented results for a wide range of values. As the valence band offset gets larger, the band gap of the superlattice decreases. This is due to the fact that the superlattice valence band is largely determined by the ZnTe

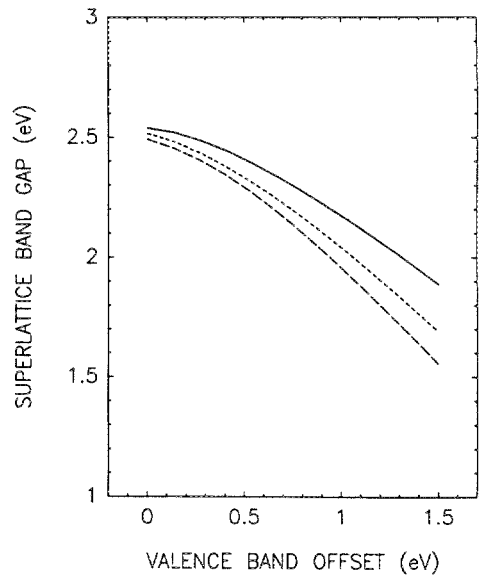

FIG. 4. Variation of the band gap of a few representative superlattices with the valence band offset $E_V^{ZnTe} - E_V^{ZnSe}$. Notice that the band gap decreases as the valence band offset is increased. The calculation includes effects due to strain. Structures were assumed to be coherently strained with an in-plane lattice constant determined by minimizing the elastic free energy of the superlattice (i.e., the free-standing limit). (——)20×20 Å, (---)15×15 Å, and (– – –)10×10 Å.

heavy hole bands while the superlattice conduction band is determined by ZnSe conduction bands. For the type II alignment of the bands that exists in this superlattice, an increase in the valence band offset brings the heavy hole band of ZnTe and the conduction band of ZnSe closer to each other, reducing the superlattice band gap. We have shown three representative superlattices corresponding to layer thicknesses of 10–10 Å, 15–15 Å, and 20–20 Å. The larger band gap is observed for the superlattice with the smallest period. This is due to the enhancement of the two-dimensional confinement of the wave functions of the superlattice as the layer thicknesses get smaller.

The $ZnSe_{1-x}Te_x$ alloy displays a large band bowing with the minimum band gap alloy occurring at $x \approx 0.65$ with a band gap of about 2.15 eV.[31,32] This implies that if the Te atoms have diffused into the ZnSe layers, the effective band edges for the superlattice would be quite different from the pure ZnTe–ZnSe system without such diffusion. In our calculations we have neglected such alloying effects, and assumed that the superlattice layers are pure ZnSe and ZnTe with sharp interfaces.

The studies by Kuwabara *et al.*[4] suggest that the superlattice photoluminescence is related to radiative recombination between band edge and localized centers, i.e., free-to-bound transitions. In ZnSe crystals doped with Te at a concentration of about 10^{18}–10^{19} cm^{-3}, one usually observes an intense emission band associated with isoelectronic centers. At this concentration of Te the band gap of ZnSe is almost unchanged. When Te is incorporated in ZnSe, there is also a tendency to form Te clusters labeled Te_n ($n \geqslant 2$). The short-range impurity potentials associated with isolated Te atoms or Te clusters can strongly localize a hole. An additional electron can then bind to this system through the Coulomb interaction. Such a system can be viewed as an exciton (*electron + hole*) bound to the isoelectronic impurity. These isoelectronic centers have remarkable quantum efficiencies ($\approx 100\%$) since these Te centers can quickly localize the minority carriers (holes) and stop them from migrating to nonradiative centers. However, in this system there is still controversy about the binding energy of the excitons at isolated Te atoms. Earlier work[33,34] implied that isolated Te_1 centers could not produce a localized state. Recent work by Yao *et al.*[35] on Te isoelectronic traps in ZnSe suggests that the Te isoelectronic states would clearly play an important role in the ZnSe–ZnTe since only a minute fraction of Te ($x \leqslant 0.01$) has to diffuse into ZnSe for levels associated with isoelectronic centers to dominate the luminescence.

We have performed a best fit to the 77 K photoluminescence of ZnSe–ZnTe superlattices and assumed that it corresponds to the 2.65 eV band observed in Te doped bulk ZnSe. However, whether the luminescence from this band is just pure Te_1 or a combination of Te_1 and higher order clusters has not been resolved yet. In this paper we have followed the notation of Yao[35] and designated this band by Te_1. Assuming that the effects of two-dimensional confinement on the bound exciton are negligible since it is tightly bound, we added this binding energy to the photoluminescence data to obtain the band gaps, and fit our calculated band gaps to the observed photoluminescence peaks from nine different superlattices. We have accounted for possible layer thickness fluctuations in these samples by allowing an uncertainty of one monolayer. The value of the valence band offset we find based on this assumption is 0.97 ± 0.10 eV. However, since the nature of the photoluminescence from these superlattices is not well understood, the significance of this number is not certain. The results of a similar analysis assuming that the photoluminescence is due to band-to-band transitions gives us 1.20 ± 0.13 eV. This prediction is about 225 meV higher than the prediction associated with bound exciton levels. If strain effects are completely neglected, the trend is to get band offsets that are higher than 1.20 eV by 100–200 meV. These calculations clearly suggest that the band alignment of the ZnSe–ZnTe superlattice is type II, with a valence band offset between ZnSe and ZnTe on the order of 1.0 eV.

Figure 5 shows a contour plot of the superlattice band gap as a function of the ZnSe and ZnTe layer thicknesses, based on a valence band offset of 0.975 eV. To obtain the actual photoluminescence energies from Fig. 5, one has to subtract the binding energy of the exciton of 160 meV. In this figure the trend is to get smaller band gaps as either the ZnSe or the ZnTe layer thickness is increased. Since the ZnSe layer acts as the barrier material for the heavy hole band, the effect it has on the valence band is quite small. Thus, changes of the band gap as layer thicknesses are varied in a direction parallel to the ZnSe axis come mainly from the motion of the conduction band. On the other hand, ZnTe acts as the barrier material for the conduction band. Thus, changes of the band gap as layer thicknesses are varied in a direction parallel to the ZnTe axis are derived mainly from the motion of the heavy hole band. This figure also shows that for superlattices of a given period ($d_{ZnSe} + d_{ZnTe} = \text{const}$), as we scan from the ZnSe side to the ZnTe side the superlattice band gap bows. This band bowing is characteristic of band structures of type II superlattices. It is interesting to note that these

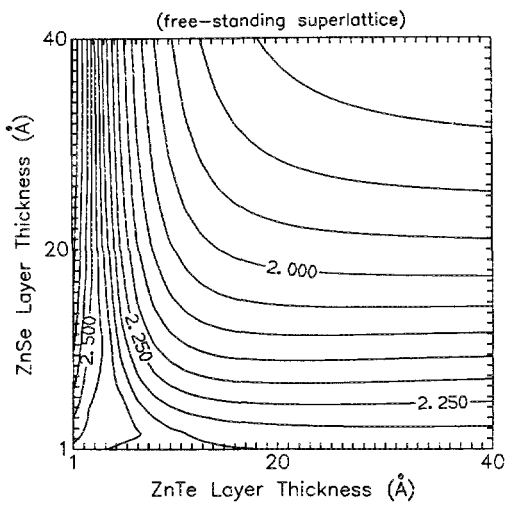

FIG. 5. Contour plot of the ZnSe–ZnTe superlattice band gap at 77 K as a function of the layer thicknesses of ZnSe and ZnTe within a single superlattice period. The valence band offset is assumed to be 0.975 eV. The lattice constants correspond to that of a free-standing superlattice. The contour interval is 50 meV. Subtracting a Te_1 bound exciton energy of 160 meV from these gaps yields energies in good agreement with observed photoluminescence peaks.

calculations for the superlattice band gap correspond well with the relatively large degree of band bowing that exists in the $ZnSe_{1-x}Te_x$ alloys.

V. CONCLUSION

We have performed detailed band structure calculations for the ZnSe–ZnTe superlattice. Currently the photoluminescence from this system seems to be due to a free to bound transition.[4] Assuming that a Te_i isoelectronic trap is responsible for the photoluminescence, we obtain a valence band offset of 0.97 ± 0.10 eV. Neglecting this binding energy gives us a band offset of 1.20 ± 0.13 eV. Hence, there is some uncertainty in the value of the valence band offset because of a lack of understanding of the source of the photoluminescence.

Our calculations indicate that it is unlikely that pure ZnSe–ZnTe superlattices would emit blue light. The efficient luminescence of these superlattices may be useful for red–green light emitters. However, substituting the pure ZnTe layers with $ZnSe_{1-x}Te_x$ layers would give blue, green, or red light depending on the alloy concentration. This remarkable degree of band gap tunability occurs within a very small range of x (alloy concentration), due to the large band bowing that occurs in these superlattices. Devices based on ZnSe–$ZnSe_{1-x}Te_x$ superlattices show definite promise for future optoelectronics.

ACKNOWLEDGMENTS

Parts of this work were supported by the Defense Advanced Research Projects Agency under Contract No. N00014-K-86-0841. We would also like to acknowledge useful discussions with T. Yao, J. O. McCaldin, P. Zampardi, and M. K. Jackson.

[1]M. Kobayashi, N. Mino, H. Katagiri, R. Kimura, M. Konagai, and K. Takahashi, J. Appl. Phys. **60**, 773 (1986).
[2]M. Kobayashi, N. Mino, H. Katagiri, R. Kimura, M. Konagai, and K. Takahashi, Appl. Phys. **48**, 296 (1986).
[3]M. Kobayashi, N. Mino, M. Konagai, and K. Takahashi, Surf. Sci. **174**, 550 (1986).
[4]H. Kuwabara, H. Fujiyasu, M. Aoki, and S. Yamada, Jpn. J. Appl. Phys. **25**, L707 (1986).
[5]H. Fujiyasu, K. Mochizuki, M. Aoki, A. Sasaki, H. Kuwabara, Y. Nakanishi, and G. Shimaoka, Surf. Sci. **174**, 543 (1986).
[6]T. Takeda, T. Kurosu, M. Lida, and T. Yao, Surf. Sci. **174**, 548 (1986).
[7]T. Yao and T. Takeda, Appl. Phys. Lett. **48**, 160 (1986).
[8]M. Kobayashi, R. Kimura, M. Konagai, and K. Takahashi, J. Cryst. Growth **81**, 495 (1987).
[9]M. Kobayashi, M. Konagai, K. Takahashi, and K. Urabe, J. Appl. Phys. **61**, 1015 (1987).
[10]Y. Rajakarunanayake, R. H. Miles, G. Y. Wu, and T. C. McGill, Phys. Rev. B (to be published).
[11]W. A. Harrison, J. Vac. Sci. Technol. **14**, 1016 (1977).
[12]P. Lawaetz, Phys. Rev. B **4**, 3460 (1971).
[13]T. Yasuda, I. Mitsuishi, and H. Kukimoto, Appl. Phys. Lett. **52**, 57 (1988).
[14]R. H. Miles, J. O. McCaldin, and T. C. McGill, J. Cryst. Growth **85**, 188 (1987).
[15]H. Asonen, J. Lilja, A. Vuoristo, M. Ishiko, and M. Pessa, Appl. Phys. Lett. **50**, 733 (1987).
[16]W. A. Harrison and J. Tersoff, J. Vac. Sci. Technol. B **4**, 1068 (1986).
[17]A. D. Katnani and G. Margaritondo, J. Appl. Phys. **54**, 2522 (1983).
[18]A. G. Milnes and D. L. Feucht, *Heterojunctions and Metal–Semiconductor Junctions* (Academic, New York, 1972).
[19]C. Van de Walle, J. Vac. Sci. Technol. B **6**, 1350 (1988).
[20]J. O. McCaldin, T. C. McGill, and C. A. Mead, Phys. Rev. Lett. **36**, 56 (1976).
[21]J. Tersoff, Phys. Rev. Lett. **56**, 2755 (1986).
[22]E. O. Kane, J. Phys. Chem. Solids **1**, 82 (1956).
[23]G. Y. Wu and T. C. McGill, Appl. Phys. Lett. **47**, 634 (1985).
[24]D. L. Smith and C. Mailhiot, Phys. Rev. B **33**, 8345 (1986).
[25]M. Aven and J. S. Prener, *Physics and Chemistry of II–VI Compounds* (North-Holland, Amsterdam, 1967).
[26]R. H. Miles, T. C. McGill, S. Sivananthan, X. Chu, and J. P. Faurie, J. Vac. Sci. Technol. B **5**, 1263 (1987).
[27]G. L. Bir and G. E. Pikus, *Symmetry and Strain Induced Effects in Semiconductors* (Keter, Jerusalem, 1974).
[28]D. L. Camphausen, G. A. N. Connell, and W. Paul, Phys. Rev. Lett. **26**, 184 (1971).
[29]A. A. Kaplyanskii and L. G. Suslina, Sov. Phys. Solid. State. **7**, 1881 (1966).
[30]D. A. Berlincourt, H. Jaffe, and L. R. Shiozawa, Phys. Rev. **129**, 1009 (1963).
[31]S. Larach, R. E. Shrader, and C. F. Stocker, Phys. Rev. **108**, 587 (1957).
[32]J. E. Bernard and A. Zunger, Phys. Rev. B **34**, 5992 (1986).
[33]W. Heimbrodt and O. Goede, Phys. Status Solidi B **135**, 795 (1986).
[34]I. V. Akimova, A. M. Aknekyan, V. I. Koziovskii, Yu. V. Korostelin, and P. V. Shapkin, Sov. Phys. Solid. State **27**, 1041 (1985).
[35]T. Yao, M. Kato, H. Tanio, and J. J. Davis, J. Cryst. Growth. **86**, 552 (1986).